MULTI-VARIATE BLOCK POLAR QUANTIZATION AND AN APPLICATION TO AUDIO

Harald Pobloth, Renat Vafin, and W. Bastiaan Kleijn

Department of Signals, Sensors, and Systems
KTH (Royal Institute of Technology)
100 44 Stockholm, Sweden
{ Harald.Pobloth, Renat.Vafin, Bastiaan.Kleijn }@s3.kth.se

ABSTRACT

In this article we introduce multi-variate block polar quantization (MBPQ). MBPQ minimizes a weighted distortion for a set of complex variables representing one block of a signal under a resolution constraint for the entire block. MBPQ allows for different probability distributions in different dimensions of the set of complex variables. It outperforms an earlier introduced block polar quantizer and unrestricted polar quantization (UPQ) both for Gaussian complex variables and for sinusoids found from audio data. In the case of audio data we found a performance gain of about 2.5 dB over the best performing conventional resolution-constrained polar quantization (UPQ).

1. INTRODUCTION

In a previous paper [1] we introduced block polar quantization (BPQ) where we considered the scalar quantization of the amplitudes and phases of a block of L sinusoids, representing a speech or audio segment of N sample length. The amplitude and phase probability density function (PDF) was assumed to be identical for all L sinusoids. In this paper we extend the BPQ method to the case where the amplitudes of all L sinusoids have different PDFs and refer to this method as multi-variate BPQ (MBPQ).

Quantization of the amplitudes and phases of complex variables (polar quantization) has found wide attention, e.g, [2–4]. One application often named is the quantization of coefficients from Fourier transforms of signals and images. Within speech and audio coding polar quantization is used in sinusoidal coding, e.g., [5, 6].

Polar quantization allows for easy facilitation of weights in the squared error criterion to account for perceptual effects. Vector quantization, which also allows weighted squared error criteria, requires search and training algorithms that impose a considerable computational effort for the high rates and dimensions typical in audio coding. On the other hand spherical quantizers, e.g., [3, 7] have been reported to outperform classical polar quantizers while maintaining low complexity. However, weighting that accounts for perceptual effects is not incorporated in these quantizers. Our results show that MBPQ outperforms other polar quantizers that easily facilitate weighting, making it an attractive quantization method in speech and audio coding.

Given a resolution constraint (a fixed bit allocation for each signal block) with a rate budget of B bits for all L amplitudes and phases, MBPQ minimizes the weighted distortion measure

$$D = \mathrm{E}\left[\frac{1}{L}\sum_{l=1}^{L} w_l \left|a_l \exp(j\phi_l) - \hat{a}_l \exp(j\hat{\phi}_l)\right|^2\right], \quad (1)$$

where $\mathrm{E}[\cdot]$ denotes expectation, w_l, a_l, and ϕ_l are the weight, amplitude, and phase of sinusoid l, respectively, the symbol $\hat{}$ indicates that the variables are quantized. Commonly the L complex variables represent a signal block of N samples, where $L < N$. In contrast to previous polar quantization methods, e.g., [3], MBPQ adapts the phase quantizers to all amplitudes observed in a block. Thus, it takes advantage of the fact that all L coefficients of a block are available to the quantizer. The weights w_l that make the distortion measure in eq. 1 perceptually meaningful can, e.g, be based on the inverse of the masking threshold. For an entropy constraint (the rate for the signal blocks varies but the average rate is fixed) this problem was earlier solved in [8].

We find that MBPQ outperforms BPQ and multi-variate unrestricted polar quantization (MUPQ) (an extension of UPQ, e.g., [3]). In UPQ the resolution of the phase quantizer in dimension l is a function of a_l. For resolution-constrained UPQ phase and amplitude are encoded with a shared index. Despite the fact that MBPQ is only asymptotically optimal, it provides good performance at practical rates. More-over the asymptotic predictions of the distortion-rate relations are useful at practical rates.

2. MULTI-VARIATE BLOCK POLAR QUANTIZATION

In this section we derive the expressions for the optimal amplitude and phase quantizers and the distortion-rate relationship of MBPQ. We assume the amplitudes of the L complex components representing a block of N data samples to be independent, and to have PDF $f_{A_l}(a)$ in dimension l. The phases are assumed to be independent identically uniformly distributed. The L amplitudes are quantized and transmitted first, and afterwards the phase quantizers in all dimensions are adapted to the observed amplitudes.

With $d(a_l, \phi_l, \hat{a}_l, \hat{\phi}_l) = \left|a_l \exp(j\phi_l) - \hat{a}_l \exp(j\hat{\phi}_l)\right|^2 = a_l^2 + \hat{a}_l^2 - 2a_l\hat{a}_l \cos(\phi_l - \hat{\phi}_l)$, the average distortion in one given quantization cell, bounded between a_{k_l} and $a_{k_l} + \Delta^a_{k_l}$ and ϕ_{i_l} and $\phi_{i_l} + \Delta^\phi_{i_l}$ is

$$D(\hat{a}_{k_l}, \hat{\phi}_{i_l}, \Delta^a_{k_l}, \Delta^\phi_{i_l}) = \frac{\int_{a=a_{k_l}}^{a_{k_l}+\Delta^a_{k_l}} \int_{\phi=\phi_{i_l}}^{\phi_{i_l}+\Delta^\phi_{i_l}} f_{A_l}(a) d(a, \hat{a}_{k_l}, \phi, \hat{\phi}_{i_l}) \mathrm{d}a\mathrm{d}\phi}{\int_{a=a_{k_l}}^{a_{k_l}+\Delta^a_{k_l}} \int_{\phi=\phi_{i_l}}^{\phi_{i_l}+\Delta^\phi_{i_l}} f_{A_l}(a) \mathrm{d}a\mathrm{d}\phi}, \quad (2)$$

This work was supported by the Swedish Research Council (Fund 271-2000-784)

where $\hat{a}_{k_l}$ is the k-th amplitude reconstruction point and $\hat{\phi}_{i_l}$ is the i-th phase reconstruction point in dimension l.

In the high-rate case, we approximate $f_{A_l}(a) \approx f_{A_l}(\hat{a}_{k_l})$ within amplitude cell k_l. Further, we assume the reconstruction points $\hat{a}_{k_l}$ and $\hat{\phi}_{i_l}$ to be the mid-points of the quantization intervals $[a_{k_l}, a_{k_l} + \Delta^a_{k_l})$ and $[\phi_{i_l}, \phi_{i_l} + \Delta^\phi_{i_l})$, respectively. In this case eq. 2 becomes independent of $\hat{\phi}_{i_l}$:

$$D(\hat{a}_{k_l}, \Delta^a_{k_l}, \Delta^\phi_{i_l}) = \frac{(\Delta^a_{k_l})^2}{12} + 2\hat{a}^2_{k_l} - 4\hat{a}^2_{k_l} \frac{\sin\left(\frac{\Delta^\phi_{i_l}}{2}\right)}{\Delta^\phi_{i_l}} . \quad (3)$$

Next we introduce the reconstruction point densities $g_{A_l}(a)$ and $g_{\Phi_l}(\hat{\mathbf{a}})$, which are the inverse of the quantization cell sizes $\Delta^a_{k_l}$ and $\Delta^\phi_{i_l}$. The phase reconstruction point density is a function of all quantized amplitudes $\hat{\mathbf{a}} = (\hat{a}_{k_1}, \dots, \hat{a}_{k_L})^T$. The independence of $g_{\Phi_l}(\hat{\mathbf{a}})$ from ϕ_l results from the uniform PDF of ϕ_l. The average distortion in a given cell becomes

$$D(\hat{a}_{k_l}, g_{A_l}(\hat{a}_{k_l}), g_{\Phi_l}(\hat{\mathbf{a}})) = \frac{g^{-2}_{A_l}(\hat{a}_{k_l})}{12} + 2\hat{a}^2_{k_l} - 4\hat{a}^2_{k_l} \frac{\sin\left(\frac{g^{-1}_{\Phi_l}(\hat{\mathbf{a}})}{2}\right)}{g^{-1}_{\Phi_l}(\hat{\mathbf{a}})} . \quad (4)$$

For high rates, we approximate the total distortion of MBPQ (D_{MBPQ}) using eqs. 4 and 1:

$$D_{MBPQ} \approx \frac{1}{L}\sum_{l=1}^{L} w_l \left[\int_{a=0}^{\infty} f_{A_l}(a)\left(\frac{g^{-2}_{A_l}(a)}{12} + 2a^2\right)\mathrm{d}a - 4\int_{\mathbf{a}=\mathbf{0}}^{\infty} \prod_{i=1}^{L} f_{A_i}(a_i) a_l^2 \sin\left(\frac{g^{-1}_{\Phi_l}(\mathbf{a})}{2}\right) g_{\Phi_l}(\mathbf{a})\mathrm{d}\mathbf{a}\right] . \quad (5)$$

In the next sections the distortion D_{MBPQ} is minimized under the constraint that we use a total of $B = B_A + B_\Phi$ bits to represent all L complex components. The amplitude and phase are represented by B_A and B_Φ bits respectively.

2.1. Amplitude reconstruction point densities

We start with observing that for a given $g_{A_l}(a)$

$$2^{B_{A_l}} = \int_{a=0}^{\infty} g_{A_l}(a)\mathrm{d}a \quad (6)$$

is equal to the number of amplitude reconstruction points in dimension l, where B_{A_l} denotes the amplitude rate budget in dimension l. Using the method of Lagrange multipliers we find the $g_{A_l}(a)$ minimizing eq. 5 for a given B_{A_l}:

$$g_{A_l}(a) = f^{1/3}_{A_l}(a) 2^{B_{A_l}} \frac{1}{\int_{a'} f^{1/3}_{A_l}(a')\mathrm{d}a'} . \quad (7)$$

Inserting eq. 7 in eq. 5 and putting a constraint on the overall amplitude rate budget $B_A = \sum_{l=1}^{L} B_{A_l}$ the individual B_{A_l} minimizing eq. 5 are given by

$$2^{B_{A_l}} = \frac{2^{B_A/L}\sqrt{w_l}}{\sqrt{\bar{w}}\prod_{n=1}^{L}\left(\int_a f^{1/3}_{A_n}(a)\mathrm{d}a\right)^{3/(2L)}} \left(\int_a f^{1/3}_{A_l}(a)\mathrm{d}a\right)^{\frac{3}{2}} , \quad (8)$$

where $\bar{w} = \prod_{n=1}^{L} w_n^{1/L}$ is the geometric mean of the weights. In case $f_{A_l}(a)$ is equal for all l we find that eqs. 8 and 7 combine to [1, eq. 13], i.e., MBPQ reduces to BPQ.

2.2. Phase reconstruction point densities

By the time the phase is to be quantized, the quantized amplitudes $\hat{\mathbf{a}}$ are known. Given $\hat{\mathbf{a}}$, the average distortion $D(\hat{\mathbf{a}})$ is found using eq. 4:

$$D(\hat{\mathbf{a}}) = \frac{1}{L}\sum_{l=1}^{L} w_l \left(\frac{g^{-2}_{A_l}(\hat{a}_{k_l})}{12} + 2\hat{a}^2_{k_l} - 4\hat{a}^2_{k_l}\frac{\sin\left(\frac{g^{-1}_{\Phi_l}(\hat{\mathbf{a}})}{2}\right)}{g^{-1}_{\Phi_l}(\hat{\mathbf{a}})}\right) . \quad (9)$$

Since $2\pi g_{\Phi_l}(\hat{\mathbf{a}})$ is the number of phase reconstruction points for dimension l, we find $g_{\Phi_l}(\hat{\mathbf{a}})$ minimizing $D(\hat{\mathbf{a}})$ under the constraint

$$B_\Phi = \sum_{l=1}^{L} \log_2\left(2\pi g_{\Phi_l}(\hat{\mathbf{a}})\right) . \quad (10)$$

Using the method of Lagrange multipliers we find

$$g_{\Phi_l}(\hat{\mathbf{a}}) = \sqrt{\frac{w_l}{\bar{w}}}\frac{\hat{a}_{k_l} 2^{B_\Phi/L}}{2\pi\prod_{n=1}^{L}\hat{a}^{1/L}_{k_n}} . \quad (11)$$

The phase quantizers $g_{\Phi_l}(\hat{\mathbf{a}})$ have to be found for each transmitted set of amplitudes. Thus, eq. 11 represents the (only) computational overhead in MBPQ compared to conventional polar quantizers, e.g., [3].

2.3. Distortion-rate relation

Using the results for B_{A_l} of eq. 8 in $g_{A_l}(a)$ of eq. 7 together with $g_{\Phi_l}(\hat{\mathbf{a}})$ in eq. 11 in the expression for the distortion given by eq. 5 we find

$$D_{MBPQ} = \frac{b}{2^{2B_A/L}} + \frac{c}{2^{2B_\Phi/L}} , \quad (12)$$

where we defined

$$b = \frac{\bar{w}}{12}\prod_{l=1}^{L}\left(\int_a f^{1/3}_{A_l}(a)\mathrm{d}a\right)^{\frac{3}{L}} ,$$

$$c = \frac{\pi^2\bar{w}}{3}\prod_{l=1}^{L}\int_a f_{A_l}(a) a^{2/L}\mathrm{d}a,$$

which are independent of the rate, and where we used the approximation $\sin(x^{-1}/2)x \approx 1/2 - x^{-2}/48$ for large x.

To find the optimal amplitude rate B_A and phase rate B_Φ for a given total rate budget $B = B_A + B_\Phi$ we denote $B_A = \alpha B$ and $B_\Phi = (1-\alpha)B$. Inserting $B_A = \alpha B$ and $B_\Phi = (1-\alpha)B$ in eq. 12 the α minimizing eq. 12 is independent of the weights:

$$\alpha = \frac{1}{2} + \frac{L}{4B}\log_2\left(\frac{b}{c}\right) . \quad (13)$$

With this α the distortion-rate relation becomes

$$D_{MBPQ} = \frac{2}{2^{B/L}}\sqrt{bc} . \quad (14)$$

Since $D_{MBPQ} \sim 2^{-B/L}$ the distortion reduces by 3 dB when B/L is increased by 1 bit.

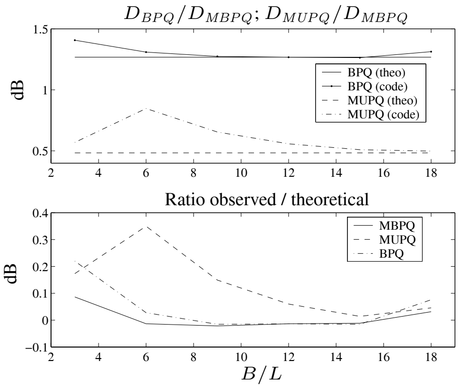

Fig. 1. Results for Gaussian data. Upper graph: Distortion ratios D_{BPQ}/D_{MBPQ}, D_{MUPQ}/D_{MBPQ} (code = observed distortions, theo = predicted distortions). Ratios greater 0 dB indicate that MBPQ is superior. Lower graph: Ratio observed and predicted distortions for MBPQ, MUPQ, and BPQ. A value greater 0 dB indicates that more distortion is observed than predicted.

3. GAUSSIAN DATA

In the literature the performance of polar quantization is often considered for the case that the real and imaginary parts of all complex components are independent Gaussian variables. This does not only lead to simple expressions but also has practical significance as argued, e.g., in [2]. The Gaussian distribution of the complex components makes the amplitudes Rayleigh distributed while the phases are uniformly distributed.

When the variance of the real and imaginary parts of the complex component in dimension l is σ_l^2 the constants b and c become

$$b = \frac{3}{8}\bar{w}\,\Gamma^3\left(\frac{2}{3}\right)\prod_{l=1}^{L}\sigma_l^{2/L}\,, \tag{15}$$

$$c = \frac{2\pi^2}{3}\bar{w}\,\Gamma^L\left(\frac{1}{L}+1\right)\prod_{l=1}^{L}\sigma_l^{2/L}\,. \tag{16}$$

As shown in, e.g., [1] unrestricted polar quantization (UPQ) [3] is a particular efficient form of polar quantization. Thus, we compare MBPQ to UPQ. In addition, we compare MBPQ and BPQ.

In resolution-constrained UPQ there is no separate quantization index for amplitude and phase and thus, it is not possible to transmit the amplitude independent of the phase. That again means it is not possible to optimize the phase density for all amplitudes observed in the current signal block. However, it is possible to optimize the UPQ in each dimension for the $f_{A_l}(a)$ in that dimension. In addition the rate budget for individual dimensions is optimized. We denote this as MUPQ. The overall MUPQ distortion becomes

$$\begin{aligned} D_{MUPQ} &= \frac{1}{L}\sum_{l=1}^{L} D_{UPQ_l} \\ &= \frac{\pi\bar{w}}{3\cdot 2^{B/L}}\prod_{l=1}^{L}\left(\int_a a^{1/2} f_{A_l}^{1/2}(a)\mathrm{d}a\right)^{\frac{2}{L}}\,, \end{aligned} \tag{17}$$

where D_{UPQ_l} is the UPQ distortion in dimension l as given[1] in [3, eq. 1]. For the Gaussian case we find

$$D_{MUPQ} = \frac{4\pi\bar{w}}{3\cdot 2^{B/L}}\prod_{l=1}^{L}\sigma_l^{2/L}\,. \tag{18}$$

We find the ratio of D_{MUPQ} and D_{MBPQ} as

$$\frac{D_{MUPQ}}{D_{MBPQ}} = \frac{4}{3}\,\Gamma^{-3/2}\left(\frac{2}{3}\right)\,\Gamma^{-L/2}\left(\frac{1}{L}+1\right), \tag{19}$$

by combining eqs. 15, 16, 14, and 18. If eq. 19 results in values larger than unity, MBPQ outperforms MUPQ. Eq. 19 is independent of the variances σ_l^2 and the rate B and it is equal to [1, eq. 29]. Thus, the results for the performance ratio between UPQ and BPQ found in [1, Figure 2] and [1, Table 1] are valid for the multivariate case as well. It should be noted however, that the ratio in eq. 19 is only obtained if either both UPQ and BPQ are assuming equal variances in all dimensions or both are adapted to the varying σ_l^2. In the limit of $L \to \infty$ we find $D_{MUPQ}/D_{MBPQ} = 1.13 \equiv 0.5280$ dB.

Figure 1 compares the predicted performance of MBPQ, BPQ, and MUPQ to each other and to the performance of actual quantizers found by averaging over the squared error from 50 000 data points. The results shown are the average for four different sets of variances $\{\sigma_l^2\}_{l=1\ldots L}$ where the σ_l^2 are uniformly distributed between 0 and 1. The dimensionality L is 40. For easy comparison we set all weights w_l to 1. The quantizers were not designed exploiting the knowledge of the Rayleigh amplitude PDF. Instead, the amplitude PDFs are found using histograms over 2 000 000 amplitude vectors (disjoint from the encoded ones) and numerical integration was used to find the reconstruction point densities. This is not necessary for the Gaussian data but it shows that the histogram method used in section 4 gives valid results.

Figure 1 shows that MBPQ outperforms BPQ by about 1.27 dB and MUPQ by about 0.5 dB. Thus, for the chosen distribution of variances the consideration of the different distributions $f_{A_l}(a)$ gives more performance advantage than the adaptation to the observed amplitudes under the erroneous assumption of identical PDFs. In other words MUPQ outperforms BPQ. However, MBPQ outperforms both.

4. AUDIO DATA

In this section, we apply MBPQ to sinusoids found using the analysis/synthesis system described in [9]. The input data are audio signals from different contemporary artists sampled at 44.1 kHz. The signals are pre-processed to remove silence intervals. We use 16.5 minutes of audio data for the estimation of the PDFs $f_{A_l}(a)$ via histograms and encode 6 minutes of audio data to find the average distortions D_{MBPQ}, D_{MUPQ}, and D_{BPQ}. For each analysis block of 10.2 ms (448 samples) a set of $L = 40$ sinusoids is extracted. The sinusoids are ordered with increasing frequency. Before encoding, the amplitudes are normalized by the maximum amplitude in the set, which has to be transmitted as side information.

In the experiments all weights w_l are set to 1. An alternative is to find weights w_l by exploiting the masking found from the amplitudes a_l as described in [8]. In this scenario the amplitude quantizers are optimized for a fixed set of w_l and the phase quantizers are optimized for the w_l found from the masking function. This way the weights are adapted to the signal and no additional side

[1] In [3] D_{UPQ} is normalized differently, which introduces a factor 2 compared to the normalization this article uses.

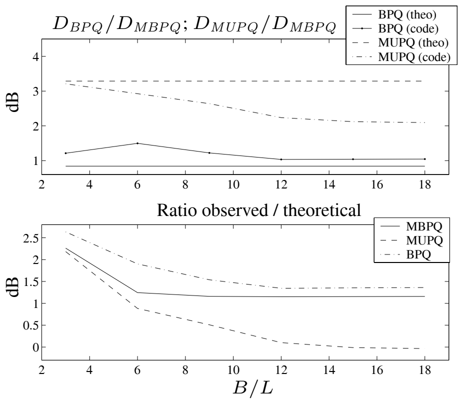

Fig. 2. Distortions in the sinusoidal components representing the audio data. Upper graph: MUPQ and BPQ compared to MBPQ (code = observed distortions, theo = predicted performance). Lower graphs: Ratio observed and predicted distortion.

information has to be transmitted. In [8] the gain from omitting the side information over-compensates the suboptimal $g_{A_l}(a)$.

In figure 2 the actual distortions observed for MBPQ, MUPQ, and BPQ quantizers are compared to the predictions of eqs. 14, 17, and [1, eq. 22]. The gain from using MBPQ instead of MUPQ for the quantization of the normalized sinusoids varies between 3.2 dB and 2.1 dB. The decrease of the performance gap with increasing rate is due to the fact that MUPQ converges exactly to its predicted behavior while MBPQ gives distortions about 1.1 dB higher than predicted, which is likely due to the very low rate in some phase quantizers. The gain of 2.1 dB corresponds to about 0.7 bits / sinusoid and relates to a rate reduction of 5.5 kbit/s for the chosen block length and 50% overlap of the blocks. The only increase in complexity to achieve this gain is the design of the phase quantizers according to eq. 11 each time the amplitudes are received. Comparing MBPQ and BPQ we see that MBPQ outperforms BPQ by about 1 dB corresponding to 2.6 kbit/s. There is no additional complexity in MBPQ compared to BPQ.

So far we considered only the distortion introduced to the sinusoidal components. Figure 3 shows the observed signal to noise ratio (SNR) in the reconstructed audio signal. The performance gain of MBPQ over MUPQ varies between 3.3 dB and 2.5 dB corresponding to about 8.6 kbit/s to 6.6 kbit/s. The gain of MBPQ over BPQ is about 1.1 dB (2.8 kbit/s). The given results consider only the distortion of the signal caused by the quantization of the sinusoidal components, not the distortion caused by the fact that the sinusoidal components do not represent the original signal without distortion. As argued in, e.g., [9], the part of the signal not captured by the sinusoids is described more efficiently by other coders, as, e.g., waveform coders.

For the audio data we observe that adapting $g_{\Phi_l}(\hat{\mathbf{a}})$ to the amplitudes observed in a signal block gives larger gain than considering the differences in the PDFs of different dimensions. This is shown by the fact that BPQ outperforms MUPQ and is the opposite of the observation for the artificial Gaussian data of section 3. Again, MBPQ performs better than both MUPQ and BPQ.

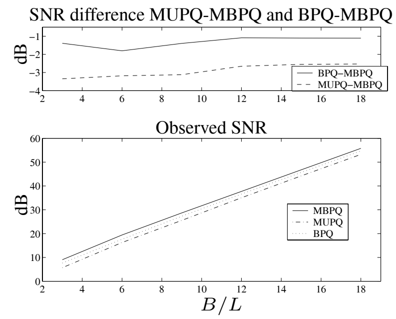

Fig. 3. SNR results for the audio signals. Upper graph: SNR in MUPQ and BPQ compared to MBPQ, values below 0 indicate better performance of MBPQ. Lower graph: Observed SNR.

5. CONCLUSIONS

Our results show that MBPQ outperforms BPQ and MUPQ. The observed reduction in rate (about 6.6 kbit/s) for audio data shows that MBPQ is useful for, e.g., sinusoidal audio coders. MBPQ is an appealing extension of BPQ and for cases where the amplitude PDF is equal in all dimensions MBPQ reduces to BPQ. The advantage over BPQ lies in the consideration of different amplitude PDFs in different dimensions and the advantage over MUPQ lies in the adaptation of the phase quantizers to all amplitudes observed in a signal block. Our results show that the relative importance of the above two advantages varies with the type of data considered.

6. REFERENCES

[1] H. Pobloth, R. Vafin, and W. B. Kleijn, "Polar quantization of sinusoids from speech signal blocks," in *Proc. Eurospeech*, September 2003, pp. 1097 – 1100.

[2] W. A. Pearlman and R. M. Gray, "Source coding of the discrete Fourier transform," *IEEE Trans. Inform. Theory*, vol. 24, no. 6, pp. 683 – 692, 1978.

[3] P. F. Swaszek and T. W. Ku, "Asymptotic performance of unrestricted polar quantizers," *IEEE Trans. Inform. Theory*, vol. 32, no. 2, pp. 330 – 333, March 1986.

[4] D. L. Neuhoff, "Polar quantization revisited," in *IEEE Int. Symp. Inform. Theory*, 1997, p. 60.

[5] K. N. Hamdy, M. Ali, and A. H. Tewfik, "Low bit rate high quality audio coding with combined harmonic and wavelet representations," in *Proc. IEEE Int. Conf. Acoust. Speech Sign. Process.*, 1996, pp. 1045 – 1048.

[6] T. S. Verma and T. H. Y. Meng, "A 6 kbps to 85 kbps scalable audio coder," in *Proc. IEEE Int. Conf. Acoust. Speech Sign. Process.*, 2000, pp. 877 – 880.

[7] J. Hamkins and K. Zeger, "Gaussian source coding with spherical codes," *IEEE Trans. Inform. Theory*, vol. 48, no. 11, pp. 2980 – 2989, 2002.

[8] R. Vafin and W. B. Kleijn, "Entropy-constrained polar quantization and its application to audio coding," *accepted, IEEE Trans. Speech Audio Proc.*, 2003.

[9] K. Vos, R. Vafin, R. Heusdens, and W. B. Kleijn, "High-quality consistent analysis-synthesis in sinusoidal coding," in *Proc. AES 17th Int. Conf., 'High-Quality Audio Coding'*, 1999, pp. 244 – 250.